Mutations targeting the plug-domain of the *Shewanella oneidensis* proton-driven stator allow swimming at increased viscosity and under anaerobic conditions

Susanne Brenzinger[1,2], Lena Dewenter[3], Nicolas J Delalez[4], Oliver Leicht[5], Volker Berndt[2], Richard M. Berry[6], Martin Thanbichler[5,7], Judith P Armitage[4], Berenike Maier[3], Kai M Thormann[1,*]

1) Justus-Liebig-Universität Gießen, Department of Microbiology and Molecular Biology at the IFZ, 35392 Gießen, Germany

2) Max-Planck-Institut für terrestrische Mikrobiologie, Department of Ecophysiology, 35043 Marburg, Germany

3) Universität Köln, Department of Physics, 50674 Cologne, Germany

4) University of Oxford, Biochemistry Department, Oxford OX1 3QU, United Kingdom

5) Philipps-Universität, Marburg, Germany LOEWE Center for Synthetic Microbiology, 35043 Marburg, Germany

6) University of Oxford, Physics Department, Oxford OX1 3QU, United Kingdom

7) Max-Planck-Institut für terrestrische Mikrobiologie & LOEWE Center für Synthetische Mikrobiologie, 35043 Marburg, Germany

Running title: MotB plug-domain mutants

Key words: flagellum, swimming, stator, torque, pmf, *Shewanella oneidensis*

*corresponding author

Kai Thormann, Justus-Liebig-Universität Gießen, Department for Microbiology and Molecular Biology at the IFZ, Heinrich-Buff-Ring 26-32, 35392 Gießen, Germany, email: kai.thormann@mikro.bio.uni-giessen.de, ++49 (0) 641 9935545, fax: ++49 (0)641 9935549

This article has been accepted for publication and undergone full peer review but has not been through the copyediting, typesetting, pagination and proofreading process which may lead to differences between this version and the Version of Record. Please cite this article as an 'Accepted Article', doi: 10.1111/mmi.13499

Summary

Shewanella oneidensis MR-1 possesses two different stator units to drive flagellar rotation, the Na^+-dependent PomAB stator and the H^+-driven MotAB stator, the latter possibly acquired by lateral gene transfer. Although either stator can independently drive swimming through liquid, MotAB-driven motors cannot support efficient motility in structured environments or swimming under anaerobic conditions. Using *ΔpomAB* cells we isolated spontaneous mutants able to move through soft agar. We show that a mutation that alters the structure of the plug domain in MotB affects motor functions and allows cells to swim through media of increased viscosity and under anaerobic conditions. The number and exchange rates of the mutant stator around the rotor were not significantly different from wild-type stators, suggesting that the number of stators engaged is not the cause of increased swimming efficiency. The swimming speeds of planktonic mutant MotAB-driven cells was reduced, and overexpression of some of these stators caused reduced growth rates, implying that mutant stators not engaged with the rotor allow some proton leakage. The results suggest that the mutations in the MotB plug domain alter the proton interactions with the stator ion channel in a way that both increases torque output and allows swimming at decreased pmf values.

Abbreviated summary

The stators of the flagellar motor are key elements with respect to motor function and properties. Here, we report that mutations affecting the so-called plug domain in MotB allow generation of higher torque and swimming under anaerobic conditions. We hypothesize that this region might be important in the functional adaptation of flagellar motors in bacteria living in different environments.

Introduction

Many bacterial species move by actively rotating flagella, long helical proteinaceous filaments extending from the cell body. Rotation of the filament is driven by the membrane-embedded motor, an intricate multiprotein complex (reviewed in (Berg, 2003)) that is powered by H^+ or Na^+ gradients. Two major components are required to convert ion fluxes into rotational movement (reviewed in (Minamino *et al.*, 2008; Sowa and Berry; 2008, Stock *et al.*, 2012)). One is the cytoplasmic rotor component referred to as the C-ring, or switch complex, which is formed by multiple copies of the proteins FliG, FliM and FliN. The second important component is the stator consisting of a variable number of stator units. These units are arranged in the cytoplasmic membrane as a ring surrounding the membrane-spanning region, the MS-ring, of the flagellar basal body. Each stator is composed of two protein subunits, commonly referred to as MotA and MotB in H^+-dependent motors and PomA and PomB in Na^+-conducting motors, in a 4A:2B stoichiometry. MotA/PomA has four transmembrane helices and is thought to interact with the C-ring component FliG via a cytoplasmic loop. MotB/PomB has a single transmembrane domain and a periplasmic region containing a peptidoglycan-binding domain that enables binding of the unit to the rigid cell wall. Two A subunits and one B subunit form a single ion-specific channel; hence, each stator unit potentially contains two ion channels (Sato and Homma, 2000a; Braun *et al.*, 2004; Kojima and Blair, 2004; Mandadapu *et al.*, 2015).

The composition of the stator ring has been shown to be highly dynamic. Stator units within the motor are constantly exchanged with a membrane-diffusing pool of stators in both MotAB (H^+-driven) and PomAB (Na^+-driven) flagellar systems. In species such as *Escherichia coli* or *Shewanella oneidensis* MR-1, up to 11 stator units can be simultaneously active within the flagellar motor to contribute to torque creation (Paulick *et al.*, 2015; Leake *et al.*, 2006; Reid *et al.*, 2006; Beeby *et al.*, 2016). However, recent studies have provided evidence that the number of stator units within Na^+- as well as within H^+-driven motors may depend on either the level of the appropriate ion motive force or the amount of load acting on the flagellar filament (Tipping *et al.*, 2013a; Tipping *et al.*, 2013b; Lele *et al.*, 2013; Fung and Berg, 1995; Sowa *et al.*, 2005; Fukuoka *et al.*, 2009). The dynamic composition of the stator ring may enable the cells to adjust flagellar functions according to environmental conditions or cellular requirements.

It is unclear how the stator units are recruited to the flagellar motor in an appropriate fashion. Each stator unit is produced as an inactive precomplex that diffuses within the cytoplasmic membrane prior to engaging with the flagellar motor. Premature ion flow through the precomplex is prevented by a periplasmic amphipathic region within the MotB protein, which is referred to as the plug domain (Hosking *et al.*, 2006; Kojima *et al.*, 2009; Li *et al.*, 2011). Only after recruitment into the flagellar motor and binding to the peptidoglycan of the cell wall does the stator becomes active, able to act as an ion channel and drive rotation of the rotor. The cytoplasmic loop within MotA as well as the C-terminal part of MotB appear to be important for functional motor-stator interactions (Kojima *et al.*, 2009; Kojima *et al.*, 2008b; Kojima *et al.*, 2008a; Hizukuri *et al.*, 2010; Morimoto *et al.*, 2010; Sato and Homma, 2000b). In addition to this basic organization the auxiliary proteins MotX and MotY have been identified as being important for the activity of Na^+-driven motors (Terashima *et al.*, 2006; Terashima *et al.*, 2010).

The challenge of proper stator acquisition is further complicated by the fact that numerous bacterial species possess two or even more distinct types of stator units to drive rotation of a single flagellar system (reviewed in (Thormann and Paulick, 2010)). The gammaproteobacterium *Shewanella oneidensis* MR-1 is motile by a single polar flagellum. In contrast to other species in its genus, *S. oneidensis* MR-1 possesses two distinct stator units to drive rotation of the single rotor (Paulick *et al.*, 2009). One of the two stators, PomAB, is conserved across all *Shewanella* species and uses Na^+ ions, whereas the second stator, MotAB, is H^+-dependent. Phylogenetic analysis of the MotAB sequence and its genetic context suggest that the encoding genes were acquired through lateral gene transfer. We have recently shown that the presence of MotAB leads to an increase of the stator exchange rate in the flagellar motor and the formation of a stator ring containing both PomAB and MotAB stators (Paulick *et al.*, 2015). Thus, the *S. oneidensis* MR-1 flagellum is probably driven by a hybrid motor whose composition is adjusted according to the environmental Na^+ concentrations. We also showed that functional rotor/stator interaction of both MotAB and PomAB stators depends on the T-ring proteins MotX and MotY, suggesting that the T-ring, not found in species with only proton-driven stators, is required to stabilize MotAB interaction in the hybrid motor (Koerdt *et al.*, 2009). Significantly, although cells with only MotAB stators can swim in liquid, they only swim for a short time and are unable to move through soft agar (Paulick *et al.*, 2009; Paulick *et al.*, 2015). When cells lacking

PomAB were incubated in soft-agar plates, mutants spontaneously arose which were able to both spread through soft agar and to swim vigorously in liquid for extended periods (Paulick *et al.*, 2009). Here, we show that this gain of function with respect to MotAB-mediated swimming is the result of mutations within the plug domain of MotB.

Results

Identification of MotB gain-of-function mutants

To isolate spontaneous mutants that display active swimming through soft agar using only MotAB stators, appropriate aliquots of a *ΔpomAB* mutant MR-1 strain were spotted on soft-agar plates. After incubation for 72 h, several colonies displayed zones of increased extension into the soft agar. Chromosomal DNA was isolated from eight individual mutants that retained this ability after several culture passages (Fig. 1A), and the gene regions encoding MotAB were sequenced. In all 8 sequences mutations in *motB* were identified. Seven mutants revealed a T to C transition in three different loci resulting in the residue substitutions Ser54Pro (3x); Ser56Pro (2x); and Leu60Ser (2x). The eighth mutant had a deletion of nine nucleotides resulting in the loss of three codons encoding residues Met47, Val48, and Glu49 (ΔMVE) from the *motB* coding sequence. Western immunoblotting with MotB antibody revealed that all mutant MotB proteins were stable, although the protein level varied among mutants even when MotB had the same substitution (Fig. 1B). While the differences in MotB concentration did not result in different movement through soft agar for the Leu60Ser mutants, the Ser54Pro MotB mutants did move further through the soft agar with increasing stator abundance (Fig. 1A).

Next, we determined whether the observed gain of function of the MotAB stator was due to the substitutions/deletions identified in *motB* and not to other secondary mutations that might have occurred elsewhere in the genome. The mutated versions of *motAB* were individually expressed from a plasmid in a *ΔpomABΔmotAB* strain (Fig. S2). Ectopic expression of all *motB* mutant variants resulted in cells which displayed motility in soft-agar plates (Fig. 1D) or when visualized microscopically (data not shown). In contrast to the mutated MotAB versions, overproduction of wild-

type MotAB did not result in elevated swimming under either condition (Fig. 1D). We thus concluded that the identified mutations in *motB* are responsible for the observed effect on swimming in the absence of PomAB.

The different protein levels of MotB protein, even in mutants bearing the same MotB variants, suggested that these differences might rather be due to an increase in gene expression rather than protein stability. To determine whether the higher MotB protein level might be caused by elevated *motAB* expression, we analyzed the *motB* transcript levels of the mutant bearing the ΔMVE deletion in MotB using a transcriptional *luxCDABE* reporter fusion (Fig. S3). Compared to the *ΔpomAB* strain, the *motB*ΔMVE variant showed increased transcription by a factor of about four which presumably accounts for the higher MotB protein level observed. In contrast, introduction of the *motB* ΔMVE allele into the chromosome of *ΔpomAB* strains resulted in MotBΔMVE production to wild-type levels as confirmed by western immunoblotting (Fig. 1C). The mutant retained the up-motile phenotype, although it was less pronounced than in the spontaneous ΔMVE mutant. This result demonstrates that the ΔMVE mutation is sufficient to cause the up-motile phenotype. Thus, a higher stator abundance caused by elevated *motAB* expression due to additional secondary mutations is not the sole cause of enhanced swimming capability of the original mutants, although it may have further increased their motility.

Mutations in a potential plug domain of MotB result in increased swimming ability

All mutations affected residues close to the periplasmic region just upstream of the MotB transmembrane domain. This region is thought to form an amphipathic helix referred to as the plug domain, which has been shown to be required to prevent premature ion flow through the stator unit in several (Fig. 2A) (Hosking *et al.*, 2006; Kojima *et al.*, 2009; Li *et al.*, 2011). However, this region in *S. oneidensis* MotB showed little homology to the same region in *E. coli* MotB, although the upstream transmembrane region is highly conserved (Fig. 2A). To determine whether this region serves as a plug domain in *S. oneidensis* MotB, we performed sequence analysis of *S. oneidensis* MotB using PSIPRED and HELIQUEST (Gautier *et al.*, 2008; Buchan *et al.*, 2013). Despite the pronounced differences in the amino acid sequence, the presence of an amphipathic helix of fifteen residues

(MotB, aa 41-55) with the characteristic distinct hydrophobic and a distinct hydrophilic side was predicted (Fig. 2A). The predicted helix encompasses the residues substituted or deleted in the MotB gain-of-function mutants, with the exception of Leu60Ser, which is three residues downstream. The gain-of-function mutations in the plug domain likely alter the helicity of the alpha helix (Ser54Pro and Ser56Pro) or the amphipathic character of this putative plug domain as predicted by PSIRED and HELIQUEST (ΔMVE, for helix-wheel projection see Fig. 2A). To test whether mutations that target this region generally lead to increased swimming of MotAB-only cells, we introduced a series of mutations into MotB (Met47Glu; Leu51Asp; Leu51Lys; Leu51Pro) which were predicted to disturb the amphipathic nature of the domain by introducing hydrophilic or hydrophobic residues or altering its helicity by a Pro substitution. All these mutations allowed some motility in soft agar, whereas amino acid substitutions which would not interfere with the amphipathic character of the region (Met47Ala, Phe46Lys) did not enable swimming through soft agar (Fig. 2B).

Overexpression of MotB proteins with substitutions that decreased the hydrophobicity of one face of the MotB plug domain of other species results in reduced growth (Hosking *et al*., 2006; Li *et al*., 2011). This result suggests that there was increased ion leakage across the cytoplasmic membrane through stators not incorporated into the flagellar motor, leading to an acidification of the cytoplasm. To test whether this was the case with the up-motile mutants, we overexpressed mutant stator genes from a plasmid and measured the growth rate of these strains (Fig. 2C; Fig. S4, Tables S1 and S2). Cells overproducing proteins mutated in position 51 (Leu51Asp, Leu51Lys, Leu51Pro) showed significantly increased doubling times. Lesser effects were seen with Leu54Pro, Leu56Pro, and Leu60Ser. As suggested by previous studies on *E. coli* MotB (Hosking *et al*., 2006), growth of the Leu51Asp mutant was restored by a secondary substitution in Asp21 (Asp21Asn), the position corresponding to Asp32 in *E. coli* MotB; this residue is critical for proton channeling. Notably, there was no statistically different change shown by any other substitution, including the MotB ΔMVE mutant which showed robust movement through soft agar.

Although there is little obvious sequence conservation between the *S. oneidensis* MR-1 and *E. coli* plug domains, these data suggest that the *S. oneidensis* MotB plug serves functions similar to those described for *E. coli* or *Vibrio* stators (Hosking *et al*., 2006; Kojima *et al*., 2009; Li *et al*., 2011). The evolutionary origin of the *S. oneidensis* MR-1 proton stators is unclear, making direct comparisons

problematic. However, the results suggest that spontaneous mutations affecting the helicity or amphipathic character of the 'plug domain' in MotB may alter the structure of the stator, with some, but not all, altering ion leakage. These changes may allow increased torque production, thus allowing movement through viscous environments. We concentrated on the mutant with the 47-49 deletion (MetValGlu; MVE) in MotB to examine the effects on the stator that led to the up-motility phenotype. This mutant produced wild-type stator levels (Fig. 1C) and had a pronounced gain-of-function phenotype with respect to motility. Furthermore, overproduction of its stators had little to no effect on growth. This mutant will henceforth be referred to as MotB* and its corresponding stator unit as MotAB*.

MotAB* exerts various effects on flagellar motor properties under planktonic conditions

To explore the properties of flagellar motors driven by the MotAB* stator unit, we first ruled out that the ΔMVE deletion would allow MotAB* to use Na^+ as coupling ion. To this end, we investigated the swimming behavior of the mutant cells in the presence of the Na^+-channel blocker phenamil. In contrast to cells propelled by PomAB-driven motors, cells solely driven by MotAB or MotAB* were unaffected by the addition of 50 μM phenamil (see Tables S3 and S4), strongly indicating that the coupling ion was not changed to Na^+ in MotAB*. We then determined the cellular swimming behavior under planktonic conditions at high (100 mM added Na^+ in LM) and low levels of Na^+ (0 mM added Na^+ in LM). Cells using only MotAB* stators (*ΔpomAB motB**) swam consistently more slowly that the MotAB-driven cells (*ΔpomAB*) under conditions of both high and low Na^+ concentrations; cells driven by wt MotAB swim at an average speed of 21.5 ± 10.9 μm · s^{-1} under high Na^+ and 19 ± 13.4 μm · s-1 under low Na^+, whereas MotAB* swam at 13.4 ± 7.0 μm · s^{-1} and 10.5 ± 5.5 μm · s^{-1} under the same conditions (Table S3 and S4). Because we have previously shown that, in *S. oneidensis* MR-1 wild-type cells, MotAB likely forms a hybrid stator ring together with Na^+-dependent PomAB stator units (Paulick *et al.*, 2015), we also determined whether MotAB* might be beneficial in the presence of PomAB. MotAB* did not change the swimming speeds compared to wt MotAB in the presence of PomAB under conditions of high (100 mM NaCl added) or low (0 mM NaCl added) concentrations of Na^+ (data not shown). In addition, we determined the average directional switching rate of the cells.

For both MotAB- and MotAB*-driven cells the rate was about 0.17 and 0.13 turns per second, respectively, values that not significantly different ($n>1100$; $p<0.05$).

To determine the effect of MotAB* on movement under more viscous conditions, we compared the swimming speed of MotAB- and MotAB*-driven cells in media in which the viscosity was increased by the addition of Ficoll (Fig. 3A, Tables S5-S7). At a concentration of 5% Ficoll, the subpopulation of motile cells was not significantly different for MotAB and MotAB* (44 ± 12 % and 41 ± 8 %, respectively), whereas in solutions containing 10% Ficoll, the subpopulation of motile MoAB cells dropped sharply (10 ± 5 %) but remained almost constant for MotAB* (40 ± 7 %). At a concentration of 12.5 % Ficoll, swimming of MotAB cells was almost completely inhibited, whereas a significant population (29 ± 8 %) of MotAB* cells still displayed robust swimming.

Thus, although cells using MotAB* stators swim more slowly, MotAB* stators allow motility under conditions of elevated viscosity without affecting the rate of directional switching. To investigate whether this was similarly true for other mutants identified during the initial screening, we determined swimming speed under normal and high viscosity conditions for the S54P (helix breaking) and L60S (affecting polarity) mutations in MotB*. We chose mutants which displayed similar MotB levels as the wild type (Fig. 1B). Both mutants gave similar results as the ΔMVE mutation with respect to motility (Tables S8 and S9). This result demonstrates that the changes in stator properties are not restricted to the ΔMVE mutant and suggests that the mutant stators either engage the rotor in increased numbers or that individual stators produce higher torque.

MotAB* mediates motility under anaerobic conditions

When quantifying the swimming speed, we constantly observed that, unlike PomAB or wt cells, MotAB cells rapidly stopped swimming, whereas cells of a MotAB*, S54P, and L60S population at a comparable density continued vigorous movement. As MotAB-driven cells swam for a longer in media with lower cell densities, we reasoned that molecular oxygen might be the limiting factor for motility.

Using an apparatus previously developed to monitor and quantify type IV pilus retraction and twitching motility while simultaneously determining the oxygen concentration, we measured the dependence of swimming motility on oxygen levels (Kurre and Maier, 2012, Dewenter *et al.*, 2015). *ΔpomAB* cells expressing wild-type MotAB or mutated MotAB* were introduced into this system at an optical density of 0.05, and the percentage of actively swimming cells and the average swimming speeds were correlated with the oxygen concentration in the medium. At oxygen saturation, wild-type MotAB mediated robust motility at an average speed of about 35 μm · s^{-1} in about 50 % of the population. The swimming speed remained relatively constant until the oxygen concentration reached about 5 μmol · l^{-1}. Between 5 and 0 μmol · l^{-1} oxygen, concentration the swimming speed rapidly dropped to below measurable levels. When cells driven by the mutated MotAB* stators were monitored, the subpopulation of actively moving cells was determined to be similar (about 47 %) to that of MotAB cells but at a lower swimming speed (about 23 μm · s^{-1}). For MotAB* cells, the swimming speed also started to drop sharply when the oxygen concentration reached 5 μmol · l^{-1}. However, the population of actively swimming cells remained constant at a speed of about 11 μm · s^{-1} even when the molecular oxygen was consumed.

These results suggest that the motility driven by MotAB stators is correlated with the amount of available molecular oxygen, and therefore probably with the proton gradient. Although the native MotAB stators stop functioning immediately when oxygen is fully depleted, the MotAB* stators continue to support motility under anaerobic conditions, suggesting that these mutant stators continue to function at lower pmf values.

MotAB and MotAB* are present in a similar stoichiometry and exchange at a similar rate

We have previously demonstrated that, at high Na^+ concentrations, 7-8 MotAB stator units are present in the S. oneidensis MR-1 flagellar motor and are constantly exchanged with stators diffusing in the membrane (Paulick *et al.*, 2015). To determine whether or not MotAB* stators engage in the motor in similar numbers and exchange at a similar rate, we used the same fluorescent microscopy approaches. We constructed mCherry fluorescent fusions to the periplasmic C-termini of MotB and MotB*, as mCherry remains fluorescent after export into the periplasm. Both *motB-mCherry* and

motB-mCherry* fusions were integrated into the chromosome of *S. oneidensis* MR-1 *ΔpomAB*, where they replaced native *motB*. The fluorescently tagged MotB/MotB* proteins were stable and supported robust motility (Fig. S5).

To determine the number of stator units within a motor, we performed stepwise photobleaching experiments on stationary fluorescent loci at the cell pole considered to be part of the flagellar motor. Under our experimental conditions, about seven MotAB stator units were found to be present in the flagellar motor (Fig. 4) which was consistent with our previous observations. Under similar conditions, the number of mutated MotAB* stator units (6-7) was determined to not be significantly different from the number of the native MotAB stator units. To quantify the extent of stator unit exchange in the flagellar motors, we performed Fluorescence Recovery After Photobleaching (FRAP) experiments on the MotB-mCherry or MotB*-mCherry clusters at the cell pole. Both mutant and non-mutant stator complexes underwent exchange within the motor, and fluorescence recovered to similar levels, indicating that the complete stator population was exchanged. The exchange of MotAB-mCherry and MotAB*-mCherry stator units occurred at a similar rate (half time of recovery for MotAB-mCherry, ~50 s; for MotAB*-mCherry, ~33 s). Taken together, these results suggest that, under our experimental conditions, both MotAB and MotAB* stator units are recruited and retained at a similar rate by the rotor. Thus, the increased ability to swim through viscous environments is not the result of increased numbers of stators engaging; the individual stators must provide increased torque.

MotXY are required for MotAB* activity

Proper stator recruitment and activity has been demonstrated to depend on several components within the flagellar motor. One of these components is the T-ring which is formed by the MotX and Y proteins in many Na^+-dependent motors, such as those of *Vibrio*, *Shewanella*, or *Aeromonas* (Terashima *et al.*, 2006; Koerdt *et al.*, 2009; Molero *et al.*, 2011). MotX and MotY are also needed for MotAB function in *S. oneidensis* (Koerdt *et al.*, 2009). However, a recent study has shown that in a PomB/MotB (PotB) chimeric protein, replacement of the C-terminal part of the PomB, including the plug domain, by the corresponding C-terminal part of MotB alleviates the requirement of the T-ring for stator function in *Vibrio alginolyticus* (Nishino *et al.*, 2015). To determine whether the altered activity of MotAB* is linked

to a change in the relationship between the stators and these ancillary proteins, *motX* and *motY* were deleted in *ΔpomAB* and *ΔpomAB motB** strains. We then examined flagellum-mediated motility of the resultant mutants. In the absence of MotX and/or MotY, neither MotAB nor the mutated MotAB* stator conferred motility on soft-agar plates or in liquid (Fig. 5). Thus, a mutation in the stator's plug domain does not alter the requirement for the T-ring for recruitment to and/or activation of MotAB the *S. oneidensis* MR-1 flagellar motor.

Discussion

It seems likely that, while PomAB is the natural stator of *S. oneidensis* MR-1, this species is evolving towards also using a proton stator, which was probably acquired by lateral gene transfer after a recent expansion to a fresh water environment. PomAB still appears to be the dominant stator, as it is able to drive flagella rotation at both low and high viscosity and under aerobic and anaerobic conditions. Although the proton-driven MotAB stators engage and can drive swimming at low viscosities, they cannot, by themselves, support swimming at high viscosity or under anaerobic conditions (Paulick *et al.*, 2015; Paulick *et al.*, 2009). Here, we describe four independent spontaneous mutants in MotB that allow movement through soft-agar plates. All of the mutations map to or close to the putative 'plug domain' in MotB identified by Hosking *et al* (Hosking *et al.*, 2006). This domain constitutes a short amphipathic helix located just downstream of the N-terminal transmembrane region, is a common feature of the MotB stator subunits. The plug domain has been shown to prevent ion leakage through unengaged stators diffusing in the membrane, with conformational changes of the MotB stator subunits, probably induced upon stator assembly into the motor, that enable both binding to the peptidoglycan cell wall and activation of the channel for ion flow (Hosking *et al.*, 2006; Kojima *et al.*, 2009; Zhu *et al.*, 2014; Kojima, 2015). Our data suggest that a similar domain is involved in controlling proton flow in *S. oneidensis* MotAB. We found that overproduction of several MotB mutant stators resulted in a significant reduction in growth rate, whereas others did not. This observation suggests that the extent to which the different mutations alter the amphipathic nature of the domain may depend on the extent of proton leakage through the free stators. This may be explained by conformational changes in MotB resulting in an altered transmembrane domain alignment which may allow some

limited ion flow prior to motor coupling while in other mutants part of the domain's amphipatic character may be retained. Notably, at normal expression levels, none of the mutations targeting the plug domain had a significant effect on growth. Mutants with the ΔMVE or Met46Glu substitution, which grew at a similar rate as wild-type strains, spread further than the mutants producing MotB altered at position Leu51, which almost completely stopped growing after induction. The different effects on growth of the different mutations suggest that increased proton leakage through stators not engaged with the rotor and increased torque generation are not necessarily correlated or, in other words, simply making the plug domain more leaky does not necessarily increase motility. Therefore, future experiments will examine how the ΔMVE mutation affects the amphipatic helix of the plug-domain without causing massive ion leakage and if shortening the plug region in other positions will result in a similar outcome. Notably, a mutation in in the plug domain of *E. coli* MotB (Tyr61) of *E. coli* MotB resulted in an up-motile phenotype when these variants were produced in stator-less *Vibrio* (Gosink and Häse, 2000). Similarly, a plug-domain mutant with an Ala57Asp substitution was found to result in a pronounced gain-of-function phenotype for a PotB (PomB/MotB) chimeric stator in *E. coli*, which contained the N-terminal 91 amino acids of PomB, including the complete plug region (Nishino *et al*., 2015). The properties of this mutant were not studied beyond showing that swimming speed of the supressor mutants exceeded that of the parent strain. However, both studies show that mutations within the plug region can positively affect stator properties in other flagellar motor systems.

The ability of MotAB* to move cells through more viscous environments than wild-type MotAB could be explained by the loose coupling model for flagellar motors (Boschert *et al*., 2015). If the mutation induces a slight conformational change in the channel that increases the pKa of the ion-binding site Asp21 in *S. oneidensis* MotB, the resulting stator could provide more torque near stall than wild-type MotAB. Following this model, a higher pKa should also result in a lower stepping rate and slower rotational speed. This prediction is also in line with our observation that MotAB*-driven cells swam significantly slower in non-viscous liquid. Similar torque-speed relationships were recently reported for an *E. coli* MotB stator variant lacking a stretch of 28 amino acids located in the periplasmic domain of MotB almost immediately downstream of the plug region (Castillo *et al*., 2013). Based on estimates of the active stator components within the motor at medium load, those authors suggested that the deletion affects the normal load-sensing mechanism that leads to an increase of active stator units upon elevated load on the filament (Lele *et al*., 2013; Tipping *et al*., 2013a). However, under our

experimental conditions, neither the number of MotAB* stator units nor the exchange rate within the motor at stall was significantly different from those of wild-type MotAB, suggesting that the ΔMVE deletion within the plug domain affects stator activity rather than stator recruitment.

The mutations in the 'plug region' of MotB also allowed flagellar rotation under anaerobic conditions. By synchronous measurements of swimming speed and the concentration of molecular oxygen we found that swimming using the wild-type MotAB stator stops when the oxygen is used up, although MotAB*-driven, and also PomAB-driven, cells continued swimming. Cells having PomAB will continue to use the sodium gradient, but cells with MotAB alone cannot use sodium ions for swimming. Lack of oxygen results in pronounced decrease in the *pmf* in *E. coli* and *Salmonella* (Setty *et al.*, 1983; Kashket, 1981), and a reduction in aerobic respiration would be expected to have the same effect on *S. oneidensis* MR-1. *S. oneidensis* has a very flexible metabolism, and it is expected that, as with other bacteria, it will maintain a low *pmf* even after oxygen has been exhausted. The continued swimming of cells with mutant stators suggests that the mutations allow continued engagement of the stator and rotor at low *pmf* levels, supporting the hypothesis that the mutations may alter the pKa of ion-binding within the stator. Further studies will be needed to show whether or not MotAB (re-)activation and function requires a certain level of *pmf* and whether the plug domain is involved in *pmf*-dependent stator activation. We showed previously that the MotAB stators require the PomAB components MotXY to function with the *S. oneidensis* MR-1 rotor. The mutant stators still require MotXY. Therefore, the increase in motor efficiency seems not to involve a change in interaction with these motor-stabilizing components.

The stator units have a major impact on the properties of the flagellar motor with respect to the coupling ion that is used for rotation and torque and speed that can be generated (reviewed in Morimoto and Minamino, 2014; Kojima, 2015). The general features of stator units, such as the domain organization of the A and B subunits and the positions of critical residues, are highly conserved among the motors of different species, irrespective of the coupling ion used. Thus, stator units or chimeras derived by joining elements of different stators are often functional when transferred into a different species and may even convert the coupling ion fueling motor rotation from Na^+ to H^+ and *vice versa* (Gosink and Häse, 2000; Asai *et al.*, 2003). It is easy to conceive that the addition of a second stator set, either through acquisition by horizontal gene transfer or formation of a paralog

system through duplication events, may be a useful asset to the existing flagellar machinery. Numerous bacterial species possess two or more distinct stator units to drive flagellar rotation (reviewed in (Thormann and Paulick, 2010)). Several lines of evidence suggest that *S. oneidensis* MR-1 has only recently acquired *motAB* by horizontal gene transfer and that the 'new' stators have not yet fully adjusted to the originally PomAB-driven flagellar motor. We, and others, have shown that single nucleotide transitions within the genes encoding the stators are sufficient to alter the flagellar motor properties significantly and are thus potentially important drivers of the functional diversification of bacterial flagellar motors.

Experimental Procedures

Bacterial strains, growth conditions, media

All strains used in this study are listed in Table S10. *Shewanella oneidensis* MR-1 (MR-1) strains were cultivated at 32°C in LB, LM100 (10 mM HEPES, pH 7.5; 100 mM NaCl; 0.02% yeast extract; 0.01% peptone; 15 mM lactate), or LM0 (LM 100 without NaCl). *Escherichia coli* strains were cultured at 37°C in LB. *E. coli* WM3064 cultures were supplemented with 2,6-diamino-pimelic acid (DAP) to a final concentration of 300μM. When necessary, 50 μg ml^{-1} kanamycin or 10% (w/v) sucrose or 1.5% (w/v) agar or 50 μM of phenamil was added to the media. Soft agar plates were prepared with LB and 0.2% (w/v) agar.

Strain constructions

Genetic manipulations of *S. oneidensis* MR-1 were always introduced into the genome to replace the native gene locus. The in-frame deletions or chromosomal integration of gene variants or fusions were obtained by sequential double homologous recombination using vector pNTPS-138-R6K carried out essentially as previously described (Lassak *et al.*, 2010). Vectors were transferred into MR-1 cells by conjugation with *E. coli* WM3064.

Vector constructions

All vectors and oligonucleotides used in this study are listed in Tables S11 and S12. Construction of the vectors was carried out using either appropriate standard restriction/ligation or Gibson assembly (Gibson *et al.*, 2009). All kits for preparation and purification of nucleic acids (VWR International GmbH, Darmstadt, Germany) and enzymes (Fermentas, St. Leon-Rot, Germany) were used according to standard manufacturers' protocols. To generate markerless in-frame deletions, 500-750 bp fragments of the up- and downstream region of a gene were combined to create a deletion leaving only eight codons of the 5'- and 3'-termini of the corresponding genes. Compared to our previous study using mCherry-fused stators (Paulick *et al.*, 2015, Paulick *et al.*, 2009), the linker region connecting MotB and mCherry was modified to improve activity of the fluorescently tagged protein. To this end MotB was fused to mCherry via a 22 amino acids long linker by amplifying *mCherry* with flanking BglII and EcoRI sites following insertion into pVENC-2 and a release of the mCherry-linked fragment by HindIII and EcoRI. The resulting fragment was subsequently joined with amplicons of the regions flanking the 3'-region of *motB* via overlap PCR. For the transcriptional *lux* reporter fusion a ~700 bp fragment upstream of *motB* including its start codon was amplified using either chromosomal DNA from wild-type or a strain carrying the ΔMVE deletion as a template and transcriptionally fused to the *luxCDABE* operon amplified from mini-Tn*7*T-Gm-*lux* (Choi *et al.*, 2005). The fusion product was ligated into pNPTS-138-R6KT. The resulting vector pNPTS-138-R6KT *PmotB luxCDABE* was transferred into the appropriate strain by conjugation and integrated into the chromosome via a single homologous recombination.

For overexpression of the *motB* variants the pBBMt vector was constructed using the pBBR1-MCS2 backbone, the promoter and multiple cloning site region were amplified from pBAD/HisA (Thermo Fisher Scientific, Waltham, USA) and the terminator region from pUC18-mini-Tn*7*T-Gm-*lux* (Choi *et al.*, 2005). Promoter/MCS and terminator fragments were amplified using primer sets B207/SH144 and B205/B206, respectively. The promoter/MCS fragment as well as pBBR1-MCS2 backbone were cut using SacI and XbaI and ligated. The resulting plasmid and the terminator fragment were subsequently digested with KpnI and PspOMI and ligated to yield pBBMt.

Determination of transcriptional levels via lux *fusions*

To determine transcriptional activity of *motB*, appropriate strains bearing the transcriptional *lux* fusion were cultivated in LM100 overnight. The following day, 1/100 dilutions of the cultures were grown to an OD600 of ~0.25. Then, 180 µl aliquots were transferred to white polystyrene plates (Greiner Bio One,

Frickenhausen, Germany), and luminescence was quantified using a Tecan Infinite M200 plate reader. Values of 6 measurements were averaged and luminescence normalized to the corresponding culture density (OD600).

Fluorescence microscopy

Prior to microscopy, strains were cultivated overnight in LM media and subcultured in LM to exponential growth phase (OD600 = 0.2 - 0.3). 4µl of culture were spotted on a PBS agarose pad (137 mM NaCl, 2.7 mM KCl, 10 mM Na2HPO4 and 1.8 mM KH2PO4, adjusted to pH 7.4 and solidified by 1% (w/v) agarose). Fluorescence images were recorded using a Leica DMI 6000 B inverse microscope (Leica, Wetzlar, Germany) equipped with an SCMOS camera (Visitron Systems, Puchheim, Germany) and a HCX PL APO 100×/1.4 objective. Image processing and analysis was carried out using the ImageJ-based Fiji tool (Schindelin *et al.*, 2012).

Motility assays

Cells of MR-1 strains from overnight cultures were used to inoculate 10 ml of LB or LM medium to an OD600 of 0.01. After reaching an OD600 of 0.2-0.3, a 50 µl aliquot was placed under a coverslip fixed by four droplets of silicone (baysilone, VWR International GmbH, Darmstadt, Germany) to generate a space of 1-2 mm height. To determine Na^+-dependent motility, LM was supplemented with 100 mM NaCl (LM100, 'high Na^+'), or 100 mM KCl (LM0, 'low Na^+'). Movies of 100 frames were taken at room temperature with a Leica DMI 6000 B inverse microscope (Leica, Wetzlar, Germany) equipped with an SCMOS camera (Visitron Systems, Puchheim, Germany) and a HCX PL APO 100×/1.4 objective. The speed of at least 150 cells per strain was quantified using the MTrackJ plugin of Fiji (Meijering *et al.*, 2012). Significance was tested using ANOVA ($p = 0.05$) in R version 3.0.1. Motility in semi-solid environments was analyzed by placing 3µl of a planktonic culture or cell material from solid plates on soft agar plates (0.2 % (w/v) agar) followed by an incubation of 24h at 30°C. Strains to be directly compared were always placed on the same plate.

Fluorescence recovery after photobleaching (FRAP)

To determine the exchange rate of stators within the flagellar motor, we used the same FRAP setup essentially as previously described (Rossmann *et al.*, 2015). Cells were cultured and immobilized on agarose pads as described above. After acquisition of a pre-bleach image a single laser pulse of 100 ms was used to bleach individual MotB-mCherry clusters. Fluorescence recovery was subsequently

monitored at 30, 60, 120, 340, 560, 780, 1000 and 1220 sec post bleaching. The integrated fluorescence intensities of the whole cell, the bleached region and a background area were measured for each time point using Fiji. After background correction, the fluorescence intensities of the bleached regions were divided by the whole cell intensity to correct for general photobleaching during the imaging process. Average values of 29 cells were plotted using OriginPro 9.1. Recovery rates were determined by fitting the data obtained for the bleached region to the single exponential function F(t) = F0*exp(-x/t1)+A where F(t) is the fluorescence at time t, A the maximum intensity, x the time in min, 1/t1 the rate constant in min^{-1} and F0 the relative fluorescence intensity at t=0 min. In all cases, fits with R2 ≥ 0.99 were obtained. Recovery half-times were calculated according to the equation τ1/2 = ln(2)*t1.

Stoichiometry

Cells from overnight cultures were used to inoculate 10 ml of LM supplemented with 100 mM KCl and adjusted to a pH of 7.3 to an OD600 of 0.05. At mid-exponential growth phase (OD600 of 0.2 – 0.3), 1 ml of cells was harvested by centrifugation and washed twice in 4M buffer (50 mM HEPES; 200 mM NaCl; 15 mM lactate, pH 7). 5µl of the suspension was spotted on an agarose pad prepared with 4M buffer. Stoichiometry of MotB stator complexes was determined essentially as described previously (Leake *et al.*, 2006, Paulick *et al.*, 2015) with the following modification: Movies of 300 frames were recorded with each frame being exposed for 0.1 s by applying a laser power of 0.1 mW with an excitation wavelength of 550 nm. Stoichiometry of MotB ΔMVE-mCherry stator was calculated by measuring initial fluorescence intensities of 450 stator cluster using ImageJ and relating them to MotB-mCherry. Statistical analyses were done using R version 3.0.1. Prior to analysis, data was log-transformed to satisfy the assumptions of homoscedasticity and normally distributed residuals. Significant differences were calculated using ANOVA ($p < 0.05$).

Oxygen-speed dependency

Measurement of oxygen concentration has been described in detail in (Kurre and Maier, 2012). In short, an oxygen sensor based on the oxygen sensitive dye Pt(II) meso-tetra(pentafluorophenyl)porphine PtTFPP (Frontier Scientific, Logan, Utah, USA) was fabricated to monitor oxygen consumption and bacterial motility simultaneously (Thomas *et al.*, 2009). The stock solution of PtTFPP (20mM in toluene) was stored at RT. PtTFPP is embedded in a Sylgard 184

polydimethylsiloxane network (PDMS, Dow Corning, Midland, Michigan, USA). Therefore, PDMS was mixed with Sylgard 184 curing agent (Ratio 10:1) and 1mM PtTFPP and directly spin-coated on cover slides to result in ~30 µm thin layers. In the end, oxygen sensors were cured at 60°C for at least 3 hours. Calibration and oxygen measurements are described in (Kurre and Maier, 2012). Images for oxygen measurements were taken every 60 s at a distance of 60 µm away from the site where the swimming speed was imaged to avoid photodamage. The swimming speed experiments were performed in a sealed chamber with a volume of 100µl in LM100-medium. The density of bacteria was adjusted to OD600 of 0.1. This density supported swimming motility while enabling undisturbed swimming and tracking. Glass slides were sealed with VALAP. The oxygen concentration at the beginning of the experiment was considered saturated, and the decrease in oxygen levels was self-mediated by the metabolic activity of the swimming cells within the system. The chamber was mounted into an inverted microscope (Nikon TI). A built-in thermobox in the microscope maintained the temperature at 30°C. Swimming speed was measured as described above.

Immunofluorescence analysis

Production and stability of MotB and its fusions were determined by immunoblot analyses. Protein lysates were prepared from exponentially growing cultures. Cell suspensions were uniformly adjusted to an OD600 of 10. Protein separation and immunoblot detection were essentially carried out as described earlier (Bubendorfer *et al.*, 2012, Binnenkade *et al.*, 2014) using polyclonal antibodies raised against mCherry (Eurogentec Deutschland GmbH, Köln, Germany) or the periplasmic part of MotB. Signals were detected using the SuperSignal® West Pico Chemiluminescent Substrate (Thermo Scientific, Schwerte, Germany) and documented using a FUSION-SL chemiluminescence imager (Peqlab, Erlangen, Germany).

Acknowledgments

The project was supported by a grant from the Deutsche Forschungsgemeinschaft (DFG) to KMT (TH831/4-1). SB was supported by the International Max Planck Research School. We are grateful to Ulrike Ruppert for technical support and Kristof Brenzinger for help with statistical analysis. NJD was funded by the EPA Cephalosporin Fund.

Author Contributions

Design of the study: SB, KMT; acquisition, analysis, and interpretation of data: SB, LD, NJD, OL, VB, RMB, MT, BM, JPA, KMT; writing of the manuscript: SB, JPA, KMT.

Conflict of interests

The authors declare no conflict of interests.

References

Asai, Y., Yakushi, T., Kawagishi, I., and Homma, M. (2003) Ion-coupling determinants of Na+-driven and H+-driven flagellar motors. *J Mol Biol* **327**: 453-463.

Beeby, M., Ribardo, D.A., Brennan, C.A., Ruby, E.G., Jensen, G.J., and Hendrixson, D.R. (2016) Diverse high-torque bacterial flagellar motors assemble wider stator rings using a conserved protein scaffold. *Proc Natl Acad Sci U S A* **113**: 1917-1926.

Berg, H.C. (2003) The rotary motor of bacterial flagella. *Annu Rev Biochem* **72**: 19-54.

Binnenkade, L., Teichmann, L., and Thormann, K.M. (2014) Iron triggers LambdaSo prophage induction and release of extracellular DNA in *Shewanella oneidensis* MR-1 biofilms. *Appl Environ Microbiol* **80**: 5304-5316.

Braun, T.F., Al-Mawsawi, L.Q., Kojima, S., and Blair, D.F. (2004) Arrangement of core membrane segments in the MotA/MotB proton-channel complex of *Escherichia coli*. *Biochemistry* **43**: 35-45.

Bubendorfer, S., Held, S., Windel, N., Paulick, A., Klingl, A., and Thormann, K.M. (2012) Specificity of motor components in the dual flagellar system of *Shewanella putrefaciens* CN-32. *Mol Microbiol* **83**: 335-350.

Buchan, D.W., Minneci, F., Nugent, T.C., Bryson, K., and Jones, D.T. (2013) Scalable web services for the PSIPRED Protein Analysis Workbench. *Nucleic Acids Res* **41**: 349-357.

Choi, K.H., Gaynor, J.B., White, K.G., Lopez, C., Bosio, C.M., Karkhoff-Schweizer, R.R., and Schweizer, H.P. (2005) A Tn*7*-based broad-range bacterial cloning and expression system. *Nat Methods* **2**: 443-448.

Dewenter, L., Volkmann, T.E., and Maier, B. (2015) Oxygen governs gonococcal microcolony stability by enhancing the interaction force between type IV pili. *Integr Biol* **7**: 1161-1170.

Fukuoka, H., Wada, T., Kojima, S., Ishijima, A., and Homma, M. (2009) Sodium-dependent dynamic assembly of membrane complexes in sodium-driven flagellar motors. *Mol Microbiol* **71**: 825-835.

Fung, D.C., and Berg, H.C. (1995) Powering the flagellar motor of *Escherichia coli* with an external voltage source. *Nature* **375**: 809-812.

Gautier, R., Douguet, D., Antonny, B., and Drin, G. (2008) HELIQUEST: a web server to screen sequences with specific alpha-helical properties. *Bioinformatics* **24**: 2101-2102.

Gibson, D.G., Young, L., Chuang, R.Y., Venter, J.C., Hutchison, C.A., 3rd, and Smith, H.O. (2009) Enzymatic assembly of DNA molecules up to several hundred kilobases. *Nat Methods* **6**: 343-345.

Gosink, K.K., and Häse, C.C. (2000) Requirements for conversion of the Na(+)-driven flagellar motor of *Vibrio cholerae* to the H(+)-driven motor of *Escherichia coli*. *J Bacteriol* **182**: 4234-4240.

Hizukuri, Y., Kojima, S., and Homma, M. (2010) Disulphide cross-linking between the stator and the bearing components in the bacterial flagellar motor. *J Biochem* **148**: 309-318.

Hosking, E.R., Vogt, C., Bakker, E.P., and Manson, M.D. (2006) The *Escherichia coli* MotAB proton channel unplugged. *J Mol Biol* **364**: 921-937.

Kashket, E.R. (1981) Effects of aerobiosis and nitrogen source on the proton motive force in growing *Escherichia coli* and *Klebsiella pneumoniae* cells. *J Bacteriol* **146**: 377-384.

Koerdt, A., Paulick, A., Mock, M., Jost, K., and Thormann, K.M. (2009) MotX and MotY are required for flagellar rotation in *Shewanella oneidensis* MR-1. *J Bacteriol* **191**: 5085-5093.

Kojima, S. (2015) Dynamism and regulation of the stator, the energy conversion complex of the bacterial flagellar motor. *Curr Opin Microbiol* **28**: 66-71.

Kojima, S., and Blair, D.F. (2004) Solubilization and purification of the MotA/MotB complex of *Escherichia coli*. *Biochemistry* **43**: 26-34.

Kojima, S., Furukawa, Y., Matsunami, H., Minamino, T., and Namba, K. (2008a) Characterization of the periplasmic domain of MotB and implications for its role in the stator assembly of the bacterial flagellar motor. *J Bacteriol* **190**: 3314-3322.

Kojima, S., Imada, K., Sakuma, M., Sudo, Y., Kojima, C., Minamino, T., *et al.* (2009) Stator assembly and activation mechanism of the flagellar motor by the periplasmic region of MotB. *Mol Microbiol* **73**: 710-718.

Kojima, S., Shinohara, A., Terashima, H., Yakushi, T., Sakuma, M., Homma, M., *et al*. (2008b) Insights into the stator assembly of the *Vibrio* flagellar motor from the crystal structure of MotY. *Proc Natl Acad Sci U S A* **105**: 7696-7701.

Kurre, R., and Maier, B. (2012) Oxygen depletion triggers switching between discrete speed modes of gonococcal type IV pili. *Biophys J* **102**: 2556-2563.

Lassak, J., Henche, A.L., Binnenkade, L., and Thormann, K.M. (2010) ArcS, the cognate sensor kinase in an atypical Arc system of *Shewanella oneidensis* MR-1. *Appl Environ Microbiol* **76**: 3263-3274.

Leake, M.C., Chandler, J.H., Wadhams, G.H., Bai, F., Berry, R.M., and Armitage, J.P. (2006) Stoichiometry and turnover in single, functioning membrane protein complexes. *Nature* **443**: 355-358.

Lele, P.P., Hosu, B.G., and Berg, H.C. (2013) Dynamics of mechanosensing in the bacterial flagellar motor. *Proc Natl Acad Sci U S A* **110**: 11839-11844.

Li, N., Kojima, S., and Homma, M. (2011) Characterization of the periplasmic region of PomB, a Na+-driven flagellar stator protein in *Vibrio alginolyticus*. *J Bacteriol* **193**: 3773-3784.

Mandadapu, K.K., Nirody, J.A., Berry, R.M., and Oster, G. (2015) Mechanics of torque generation in the bacterial flagellar motor. *Proc Natl Acad Sci U S A* **112**: 4381-4389.

Meijering, E., Dzyubachyk, O., and Smal, I. (2012) Methods for cell and particle tracking. *Methods Enzymol* **504**: 183-200.

Minamino, T., Imada, K., and Namba, K. (2008) Molecular motors of the bacterial flagella. *Curr Opin Struct Biol* **18**: 693-701.

Molero, R., Wilhelms, M., Infanzon, B., Tomas, J.M., and Merino, S. (2011) *Aeromonas hydrophila motY* is essential for polar flagellum function, requires coordinate expression of *motX* and Pom proteins. *Microbiology* **157**: 2772-27784.

Morimoto, Y.V., and Minamino, T. (2014) Structure and function of the bi-directional bacterial flagellar motor. Biomolecules **4**: 217-234.

Morimoto, Y.V., Nakamura, S., Kami-ike, N., Namba, K., and Minamino, T. (2010) Charged residues in the cytoplasmic loop of MotA are required for stator assembly into the bacterial flagellar motor. Mol Microbiol **78**: 1117-1129.

Nishino, Y., Onoue, Y., Kojima, S., and Homma, M. (2015) Functional chimeras of flagellar stator proteins between *E. coli* MotB and Vibrio PomB at the periplasmic region in *Vibrio* or *E. coli*. MicrobiologyOpen **4**: 323-331.

Paulick, A., Delalez, N.J., Brenzinger, S., Steel, B.C., Berry, R.M., Armitage, J.P., and Thormann, K.M. (2015) Dual stator dynamics in the *Shewanella oneidensis* MR-1 flagellar motor. Mol Microbiol **96**: 993-1001.

Paulick, A., Koerdt, A., Lassak, J., Huntley, S., Wilms, I., Narberhaus, F., and Thormann, K.M. (2009) Two different stator systems drive a single polar flagellum in *Shewanella oneidensis* MR-1. Mol Microbiol **71**: 836-850.

Reid, S.W., Leake, M.C., Chandler, J.H., Lo, C.J., Armitage, J.P., and Berry, R.M. (2006) The maximum number of torque-generating units in the flagellar motor of *Escherichia coli* is at least 11. Proc Natl Acad Sci U S A **103**: 8066-8071.

Rossmann, F., Brenzinger, S., Knauer, C., Dörrich, A.K., Bubendorfer, S., Ruppert, U., *et al*. (2015) The role of FlhF and HubP as polar landmark proteins in *Shewanella putrefaciens* CN-32. Mol Microbiol **98**: 727-742.

Sato, K., and Homma, M. (2000a) Functional reconstitution of the Na(+)-driven polar flagellar motor component of *Vibrio alginolyticus*. J Biol Chem **275**: 5718-5722.

Sato, K., and Homma, M. (2000b) Multimeric structure of PomA, a component of the Na^+-driven polar flagellar motor of *Vibrio alginolyticus*. J Biol Chem **275**: 20223-20228.

Schindelin, J., Arganda-Carreras, I., Frise, E., Kaynig, V., Longair, M., Pietzsch, T., *et al*. (2012) Fiji: an open-source platform for biological-image analysis. Nat Methods **9**: 676-682.

Setty, O.H., Hendler, R.W., and Shrager, R.I. (1983) Simultaneous measurements of proton motive force, delta pH, membrane potential, and H+/O ratios in intact *Escherichia coli*. Biophys J **43**: 371-381.

Sievers, F., Wilm, A., Dineen, D., Gibson, T.J., Karplus, K., Li, W., *et al.* (2011) Fast, scalable generation of high-quality protein multiple sequence alignments using Clustal Omega. Mol Syst Biol **7**: 539.

Sowa, Y., and Berry, R.M. (2008) Bacterial flagellar motor. Q Rev Biophys **41**: 103-132.

Sowa, Y., Rowe, A.D., Leake, M.C., Yakushi, T., Homma, M., Ishijima, A., and Berry, R.M. (2005) Direct observation of steps in rotation of the bacterial flagellar motor. Nature **437**: 916-919.

Stock, D., Namba, K., and Lee, L.K. (2012) Nanorotors and self-assembling macromolecular machines: the torque ring of the bacterial flagellar motor. Curr Opin Biotechnol **23**: 545-554.

Terashima, H., Fukuoka, H., Yakushi, T., Kojima, S., and Homma, M. (2006) The *Vibrio* motor proteins, MotX and MotY, are associated with the basal body of Na^+-driven flagella and required for stator formation. Mol Microbiol **62**: 1170-1180.

Terashima, H., Koike, M., Kojima, S., and Homma, M. (2010) The flagellar basal-body associated protein, FlgT, essential for a novel ring structure in sodium-driven *Vibrio* motor. J Bacteriol **192**: 5609-5615.

Thomas, P.C., Halter, M., Tona, A., Raghavan, S.R., Plant, A.L., and Forry, S.P. (2009) A noninvasive thin film sensor for monitoring oxygen tension during in vitro cell culture. Anal Chem **81**: 9239-9246.

Thormann, K.M., and Paulick, A. (2010) Tuning the flagellar motor. Microbiology **156**: 1275-1283.

Tipping, M.J., Delalez, N.J., Lim, R., Berry, R.M., and Armitage, J.P. (2013a) Load-dependent assembly of the bacterial flagellar motor. MBio **4**, doi: 10.1128/mBio.00551-13.

Tipping, M.J., Steel, B.C., Delalez, N.J., Berry, R.M., and Armitage, J.P. (2013b) Quantification of flagellar motor stator dynamics through in vivo proton-motive force control. Mol Microbiol **87**: 338-347.

Zhu, S., Takao, M., Li, N., Sakuma, M., Nishino, Y., Homma, M., *et al*. (2014) Conformational change in the periplamic region of the flagellar stator coupled with the assembly around the rotor. Proc Natl Acad Sci U S A **111**: 13523-13528.

Figure legends

Figure 1: Characterization of point mutations in the plug domain of MotB.

A) Soft-agar swimming assays of the wild type (wt) and spontaneous mutants harboring an amino acid substitution in MotB, as indicated. B) Production of MotB variants in spontaneous mutants. An immunoblot analysis of MotB production by the wild type, control strains (Δ*motAB* and Δ*pomAB*) and the spontaneous mutants is shown. The antibody was raised against *S. oneidensis* MotB. The arrows point to the position corresponding to the estimated molecular mass of MotB according to the missing band in the *ΔmotAB* control lane. See Fig. S1 for the corresponding loading control. The additional bands stem from unspecific cross reactions of the antibody with other proteins. C) Production of MotB in a defined ΔMVE mutant. Shown is an immunoblot analysis of MotB production by the wild type, control strains (Δ*motAB* and Δ*pomAB*), the spontaneous ΔMVE mutant (sp.), and the mutant with an introduced ΔMVE deletion (ins.). The arrow points to the position corresponding to the estimated molecular mass of MotB according to the missing band in the *ΔmotAB* control lane. See Fig. S1 for the corresponding loading control. The additional bands stem from unspecific cross reactions of the antibody with other proteins. Right panel: Soft-agar swimming assay of the wild type and the mutants harboring the spontaneous (sp.) or the introduced (ins.) ΔMVE deletion. D) Soft agar assay of wild-type and *ΔpomABΔmotAB* mutant cells overproducing either wild-type MotAB or mutant versions from a plasmid under the control of an arabinose-inducible promoter. Corresponding immunoblot analysis of MotB production of these strains is shown in Fig. S2. Note that each soft-agar plate experiment is depicted at an individual scale. Therefore, every experiment has its own wild-type control. All soft agar assays were performed by placing small amounts of cells from plates on 0.2 % soft-agar plates and followed by incubation at 30 °C for 24 h prior documentation of the lateral extension zones. Dashed lines indicate rearrangement of the original positions on the same soft-agar plate to allow a better comparison in the figure.

Figure 2: Analysis of the plug domain mutants.

A) Schematic illustration of the MotAB stator and its plug domain (colored barrel). Image at the right shows a helical wheel projection of the plug domain looking up from the membrane. Yellow circles

represent hydrophobic residues, blue circles represent positively charged, red circles represent negatively charged amino acids, and grey circles representing polar uncharged residues. All amino acids targeted in this study are indicated by their residue number. The lower helical wheel projection shows the predicted arrangement of amino acids in the plug domain of MotB ΔMVE mutant. An alignment of the amino acid sequences encompassing the predicted transmembrane and plug domains of *E. coli* and *S. oneidensis* MotB illustrates the highly conserved amino acids around the ion binding residue (grey box) and the low homology between the plug-domains (yellow boxes). Grey arrows indicate the last amino acid of the predicted transmembrane region (TM), and black arrows point to functionally crucial residues for *E. coli* MotB and the substituted or deleted residues of MR-1 MotB. Positions of residues that are identical in the two sequences are indicated by an asterisk, and colons mark positions at which amino acids are chemically conserved. Sequences were aligned using Clustal Omega (Sievers *et al.*, 2011). B) Soft-agar assay of an MR-1 EV control and MR-1 Δ*pomAB* Δ*motAB* mutants producing either wild-type MotAB or MotB mutant versions from the pBBMt plasmid under the control of an arabinose-inducible promoter. EV = empty-vector control. Dashed lines indicate rearranged lateral extension zones from the same soft-agar plate. C) Growth curves of MR-1 EV and MR-1 Δ*pomAB* Δ*motAB* strains harboring the indicated *motAB* variants on a plasmid under the control of an arabinose-inducible promoter. Curves of cultures that were induced by the addition of 0.2% arabinose (w/v) at time point 0 (black arrow) are indicated with an “i”. For growth experiments of further strains and a list of doubling times refer to Fig. S4 and table S1. EV = empty-vector control.

Figure 3: Motile fraction and swimming speeds at elevated viscosity.

The motile fraction of cells expressing either MotAB (grey bars) or MotAB* (white bars) in a Δ*pomAB* background strain were determined in LB broth containing 5, 10 or 12.5% (w/v) Ficoll (A) or in LM100 with saturated or depleted oxygen concentrations (B). The asterisks and bars indicate the subpopulations of motile cells [%] that were significantly different from each other ($p<0.05$). The average swimming speed of each strain under each condition is indicated in the corresponding bar. With the exception of speed of MR-1 Δ*pomAB motB* supplemented with 12.5% (w/v) Ficoll, all average speeds were calculated from at least 100 cells.

Figure 4: Quantity and exchange halt time of MotAB and MotAB*.

Left panel: quantification of single MotB (grey bar) or MotB* (white bar) subunits fused to mCherry. The number of single MotBmCherry molecules was calculated by the number of distinct steps in intensity loss during continuous photobleaching. The number of MotB*mCherry molecules peresent in the motor was calculated by comparison of the initial fluorescence intensities of stator clusters formed by MotBmCherry and MotB*mCherry. Error bars represent the standard deviation, n=450. Right panel: Normalized averaged fluorescence intensity as a function of time obtained from a FRAP analysis of MotBmCherry (solid black square and solid line) and MotB*mCherry (open triangle and dashed line). The half times of recovery (τ ½) were calculated by fitting an exponential decay to the averaged normalized fluorescence intensity of clusters in 29 cells. Error bars indicate the standard error of the mean. mC = mCherry.

Figure 5: Role of MotXY in motility powered by MotAB and MotAB*.

Soft-agar assay of wild-type (wt), MR-1Δ*pomAB motB* and MR-1Δ*pomAB motB** combined with deletions of *motX* and *motY*. Cells of liquid cultures were spotted on soft-agar plates containing 0.25% (w/v) agar and incubated for 24h at 30°C prior to measurement of radial extensions. All strains right from the dashed line carry a deletion of *pomAB*.

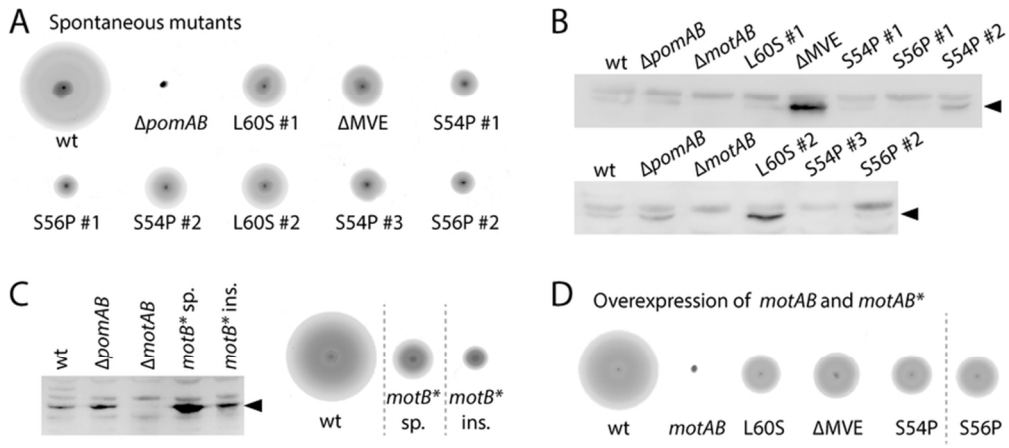

Figure 1: Characterization of point mutations in the plug domain of MotB.
A) Soft-agar swimming assays of the wild type (wt) and spontaneous mutants harboring an amino acid substitution in MotB, as indicated. B) Production of MotB variants in spontaneous mutants. An immunoblot analysis of MotB production by the wild type, control strains (ΔmotAB and ΔpomAB) and the spontaneous mutants is shown. The antibody was raised against S. oneidensis MotB. The arrows point to the position corresponding to the estimated molecular mass of MotB according to the missing band in the ΔmotAB control lane. See Fig. S1 for the corresponding loading control. The additional bands stem from unspecific cross reactions of the antibody with other proteins. C) Production of MotB in a defined ΔMVE mutant. Shown is an immunoblot analysis of MotB production by the wild type, control strains (ΔmotAB and ΔpomAB), the spontaneous ΔMVE mutant (sp.), and the mutant with an introduced ΔMVE deletion (ins.). The arrow points to the position corresponding to the estimated molecular mass of MotB according to the missing band in the ΔmotAB control lane. See Fig. S1 for the corresponding loading control. The additional bands stem from unspecific cross reactions of the antibody with other proteins. Right panel: Soft-agar swimming assay of the wild type and the mutants harboring the spontaneous (sp.) or the introduced (ins.) ΔMVE deletion. D) Soft agar assay of wild-type and ΔpomABΔmotAB mutant cells overproducing either wild-type MotAB or mutant versions from a plasmid under the control of an arabinose-inducible promoter. Corresponding immunoblot analysis of MotB production of these strains is shown in Fig. S2. Note that each soft-agar plate experiment is depicted at an individual scale. Therefore, every experiment has its own wild-type control. All soft agar assays were performed by placing small amounts of cells from plates on 0.2 % soft-agar plates and followed by incubation at 30 °C for 24 h prior documentation of the lateral extension zones. Dashed lines indicate rearrangement of the original positions on the same soft-agar plate to allow a better comparison in the figure.

74x32mm (300 x 300 DPI)

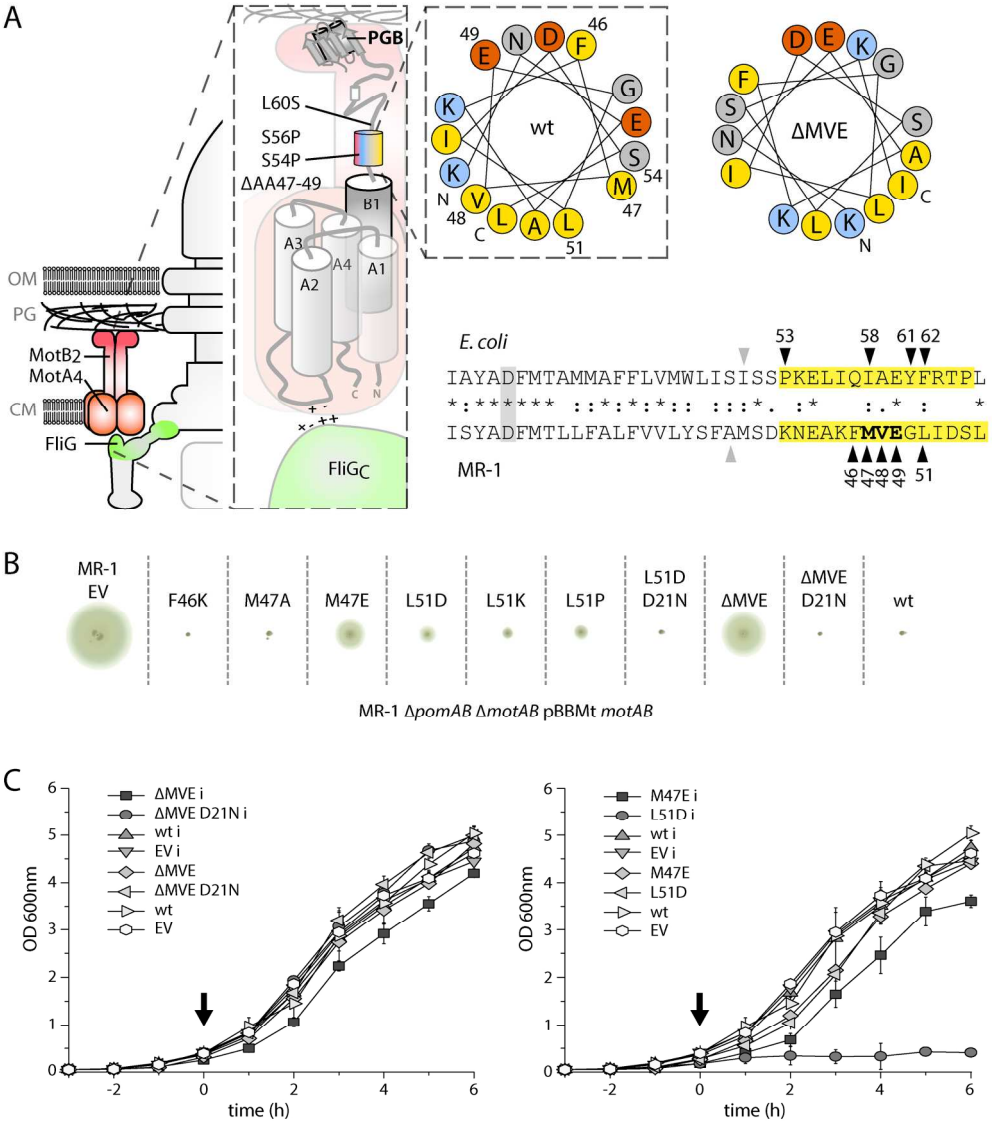

Figure 2: Analysis of the plug domain mutants.
A) Schematic illustration of the MotAB stator and its plug domain (colored barrel). Image at the right shows a helical wheel projection of the plug domain looking up from the membrane. Yellow circles represent hydrophobic residues, blue circles represent positively charged, red circles represent negatively charged amino acids, and grey circles representing polar uncharged residues. All amino acids targeted in this study are indicated by their residue number. The lower helical wheel projection shows the predicted arrangement of amino acids in the plug domain of MotB ΔMVE mutant. An alignment of the amino acid sequences encompassing the predicted transmembrane and plug domains of E. coli and S. oneidensis MotB illustrates the highly conserved amino acids around the ion binding residue (grey box) and the low homology between the plug-domains (yellow boxes). Grey arrows indicate the last amino acid of the predicted transmembrane region (TM), and black arrows point to functionally crucial residues for E. coli MotB and the substituted or deleted residues of MR-1 MotB. Positions of residues that are identical in the two sequences are indicated by an asterisk, and colons mark positions at which amino acids are chemically conserved. Sequences were aligned using Clustal Omega (Sievers et al., 2011). B) Soft-agar assay of an MR-1 EV control and MR-1 ΔpomAB ΔmotAB mutants producing either wild-type MotAB or MotB mutant versions from the pBBMt plasmid under the control of an arabinose-inducible promoter. EV = empty-vector control. Dashed lines

indicate rearranged lateral extension zones from the same soft-agar plate. C) Growth curves of MR-1 EV and MR-1 ΔpomAB ΔmotAB strains harboring the indicated motAB variants on a plasmid under the control of an arabinose-inducible promoter. Curves of cultures that were induced by the addition of 0.2% arabinose (w/v) at time point 0 (black arrow) are indicated with an "i". For growth experiments of further strains and a list of doubling times refer to Fig. S4 and table S1. EV = empty-vector control.

188x213mm (300 x 300 DPI)

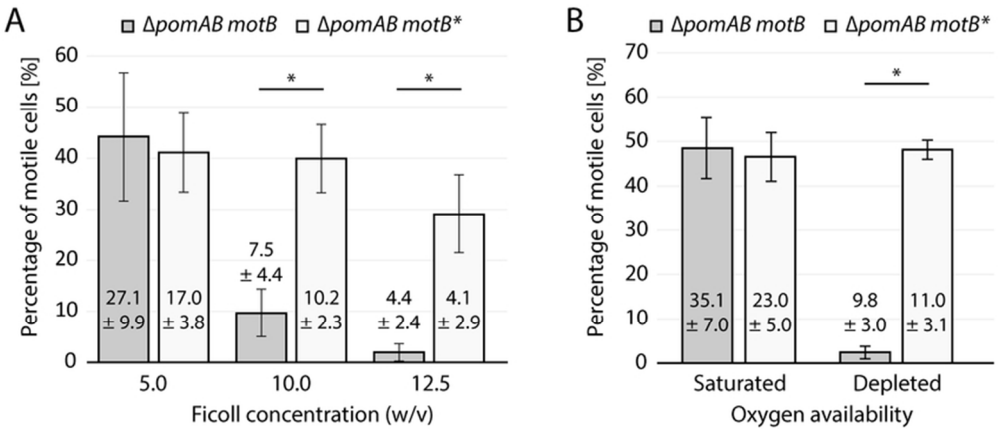

Figure 3: Motile fraction and swimming speeds at elevated viscosity.
The motile fraction of cells expressing either MotAB (grey bars) or MotAB* (white bars) in a ΔpomAB background strain were determined in LB broth containing 5, 10 or 12.5% (w/v) Ficoll (A) or in LM100 with saturated or depleted oxygen concentrations (B). The asterisks and bars indicate the subpopulations of motile cells [%] that were significantly different from each other ($p<0.05$). The average swimming speed of each strain under each condition is indicated in the corresponding bar. With the exception of speed of MR-1 ΔpomAB motB supplemented with 12.5% (w/v) Ficoll, all average speeds were calculated from at least 100 cells.

71x30mm (300 x 300 DPI)

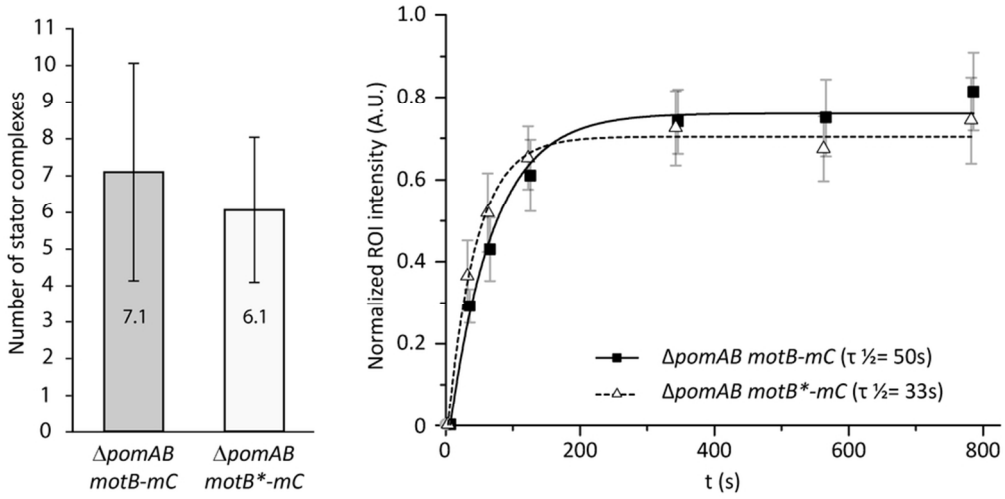

Figure 4: Quantity and exchange halt time of MotAB and MotAB*.
Left panel: quantification of single MotB (grey bar) or MotB* (white bar) subunits fused to mCherry. The number of single MotBmCherry molecules was calculated by the number of distinct steps in intensity loss during continuous photobleaching. The number of MotB*mCherry molecules peresent in the motor was calculated by comparison of the initial fluorescence intensities of stator clusters formed by MotBmCherry and MotB*mCherry. Error bars represent the standard deviation, n=450. Right panel: Normalized averaged fluorescence intensity as a function of time obtained from a FRAP analysis of MotBmCherry (solid black square and solid line) and MotB*mCherry (open triangle and dashed line). The half times of recovery (τ ½) were calculated by fitting an exponential decay to the averaged normalized fluorescence intensity of clusters in 29 cells. Error bars indicate the standard error of the mean. mC = mCherry.

84x42mm (300 x 300 DPI)

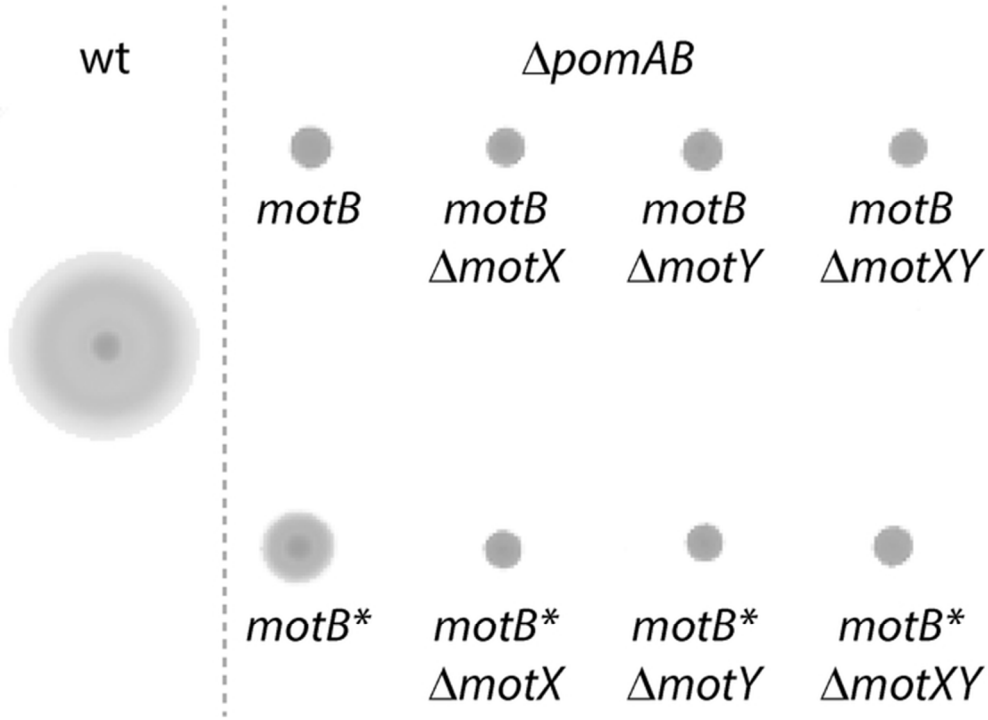

Figure 5: Role of MotXY in motility powered by MotAB and MotAB*.
Soft-agar assay of wild-type (wt), MR-1ΔpomAB motB and MR-1ΔpomAB motB* combined with deletions of motX and motY. Cells of liquid cultures were spotted on soft-agar plates containing 0.25% (w/v) agar and incubated for 24h at 30°C prior to measurement of radial extensions. All strains right from the dashed line carry a deletion of pomAB.

58x42mm (300 x 300 DPI)

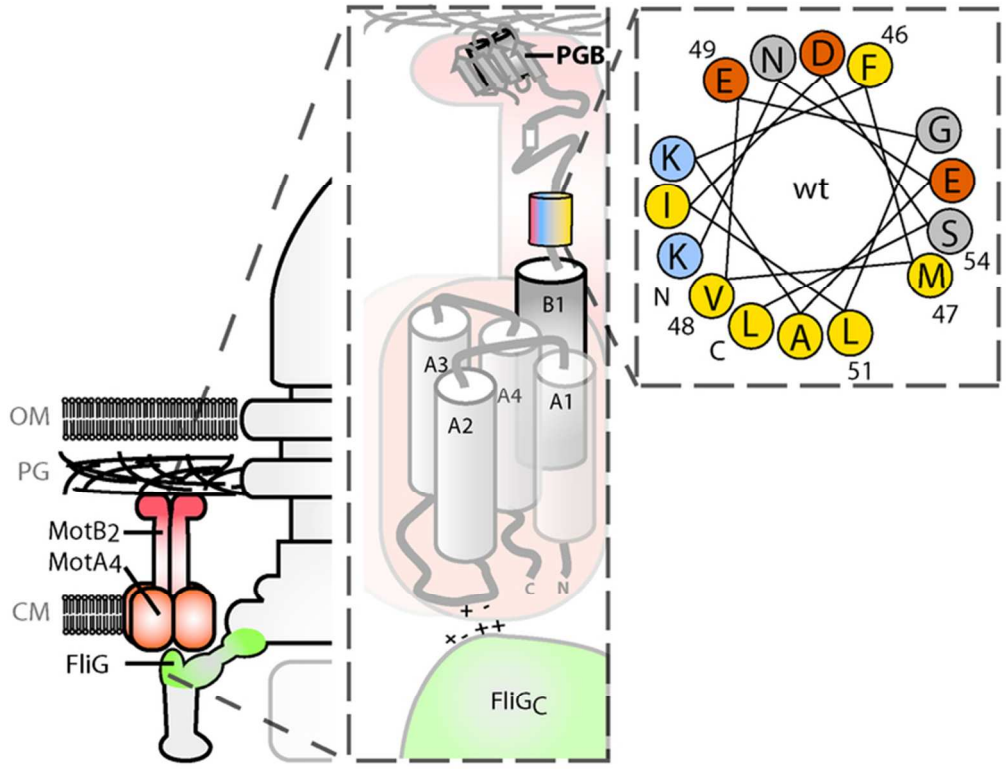

The stators of the flagellar motor are key elements with respect to motor function and properties. Here, we report that mutations affecting the so-called plug domain in MotB allow generation of higher torque and swimming under anaerobic conditions. We hypothesize that this region might be important in the functional adaptation of flagellar motors in bacteria living in different environments.

65x53mm (300 x 300 DPI)

Abbreviated summary

The stators of the flagellar motor are key elements with respect to motor function and properties. Here, we report that mutations affecting the so-called plug domain in MotB allow generation of higher torque and swimming under anaerobic conditions. We hypothesize that this region might be important in the functional adaptation of flagellar motors in bacteria living in different environments.